Chapter 17
Optimization of Flatbed UV-Printed Digital Image Correlation Speckle Patterns for Microscale Strain Mapping

Aastha S. Singh, Aaron P. Stebner, and Zachary D. Brunson

Abstract Digital image correlation (DIC), an optical method of measuring full-field deformation, relies on the use of applied speckle patterns to track strain, with the quality of the pattern directly influencing the error and variability of the results. Traditional methods of pattern generation lack the resolution and control necessary to pattern small samples, but using UV printers to print computer-generated speckle patterns may offer a solution, seeing that the placement, size, and shape of speckles can be precisely controlled. A computational study was run to investigate how these parameters affect the performance of the pattern under a variety of different tensile, compressive, and shear strain states. Results indicate that irregularly shaped speckles with some randomness provide the most accurate and consistent patterns with which to measure axial strain, but no pattern was able to correctly convey shear strain. Randomness in speckle placement was found to influence precision more than accuracy, seeing that grid-like patterns with no positional randomness had significant variability. UV printing these patterns reveals that imperfections caused by the spreading of printer ink before curing may introduce enough inherent randomness to make positional randomness redundant.

Keywords DIC · Speckle Pattern · Randomness · Repeatability

Introduction & Background

Digital image correlation (DIC) is a non-contact method of measuring strain in which a pattern of dots, called a speckle pattern, is applied to a specimen and digital image registration is used to track the movement and deformation of the dots as the specimen undergoes deformation. By tracking sub-regions of the speckle patterns, called subsets, and comparing them to prior and future pattern images, a full-field strain measurement of the specimen may be obtained with the assumption that the pattern and the specimen are fully bonded and move as one body [1, 2]. DIC is used to examine a multitude of materials, including metals, plastics, composites, and biological materials, under both quasi-static and dynamic loading conditions, steadily replacing other techniques such as various interferometry techniques and other optical methods, such as Moiré patterns [3].

The performance of DIC measurements often rests on factors relating to the speckle pattern itself [4, 5]. The orientation and distribution of the speckles, or the randomness of their placement, is often a key factor in creating a high-quality pattern – uniform grids of patterns often result in false matching, due to correlation software mistaking strain for rigid body motion when tracking the movement of a speckle. However, too much randomness may result in large uniform black or white regions, leading to areas of data loss. Speckle density is also considered, with a 50% coverage being considered ideal to maximize contrast and data collection points [1, 6, 7]. Speckles themselves should be around 3-5 camera pixels across – sizing speckles too small leads to data loss from lack of camera resolution and sizing them too large leads to unnecessary data collection, taking up processing time and storage space. Pixels may also be susceptible to bleeding light into neighboring

Aastha S. Singh · Zachary D. Brunson (✉)
George W. Woodruff School of Mechanical Engineering, Georgia Institute of Technology, 801 Ferst Dr. Atlanta, GA 30318
e-mail: asingh913@gatech.edu; zachary.brunson@me.gatech.edu

Aaron P. Stebner
George W. Woodruff School of Mechanical Engineering, Georgia Institute of Technology, 801 Ferst Dr. Atlanta, GA 30318
School of Materials Science and Engineering, Georgia Institute of Technology, 801 Ferst Dr. Atlanta, GA 30318
e-mail: aaron.stebner@gatech.edu

Kristin B. Zimmerman, PhD (eds.), *Computer Vision and SLDV for Structural Dynamics, 2026, Vol. 6*, Conference Proceedings of the Society for Experimental Mechanics Series, https://doi.org/10.1007/978-8-743-81445-0_17

pixels the smaller they get, so subsets that are smaller than necessary may increase error without benefit. The subset size is crucial to the accuracy of the strain measurement as well. Subsets that are too small risk not having enough information to differentiate themselves from neighboring subsets, or even not having enough information to differentiate displacement. Conversely, overly large subsets result in deformation information being averaged over a larger area, making displacement gradients more difficult to discern. Both result in poor strain measurements and high error [1, 6–8].

Traditional DIC pattern techniques include spray paint, rollers, or colored powders applied randomly to specimen surfaces, with the most accurate and viable methods being paint- or ink-based [8, 9]. While traditional DIC patterning techniques are sufficient for larger samples, standard DIC systems are not able to conduct measurements on samples smaller than 10mm without specialized microscopes [10]. For materials that are expensive, delicate, or difficult to manufacture, testing large samples of materials may be costly or extremely difficult, so traditional DIC methods may not be a feasible option for testing, seeing that traditional speckle creation methods lack the precision and resolution necessary for reliable analysis at small scales. Traditional methods struggle to achieve speckle uniformity and often push specimen coverage well beyond the ideal 50% threshold, due to an inability to control speckle size, while novel methods of printing optimized patterns directly onto samples yield much better accuracy and precision [8, 9].

Currently, there is no method to generate highly controlled and repeatable speckle patterns, but utilizing UV printers may be able to address this gap by creating patterns with precise control over parameters like speckle size, density, and placement [9, 11]. In addition to optimizing these parameters, UV printers offer the possibility of creating patterns that are isotropic and scaled to match the gauge size of any given specimen, including ones smaller than 10mm. Research looking into engineered patterns is sparse and UV printing for DIC applications has been seldom explored. In one of the few studies in which UV printed patterns were appraised, the patterns yielded were deemed to be too large to analyze [11, 12].

While prior work has explored the feasibility of using DIC to measure deformation at micro-scales and the performance of computer-generated DIC patterns, no study has examined the merits of computer-generated UV-printed DIC speckle patterns [11, 12]. Thus, this study endeavors to (1) evaluate whether UV-printed patterns can accurately track deformation in small specimen while (2) examining the tradeoff between controlling patterning and randomness to improve data density, improve measurement accuracy, and reduce error or data loss.

Modeling Methodology

To simulate UV printed speckles prior to physical experiments, a computational study was run to evaluate how different parameters affect the performance of speckle patterns. A MATLAB script was developed to create and deform the speckle patterns under seven different applied strain states.

Pattern dimensions were set to be 4.5 mm × 1.8 mm, corresponding to the planned gauge size of future experimental follow-up investigations. The patterns were designed to fit the resolution capability of a Roland VersaUV LEF-12i Benchtop UV Flatbed Printer, which has a printing resolution of up to 1440 × 720 dots-per-inch, corresponding to planned future experiments [13]. These constraints were used to select the speckle density and theoretical camera magnification. In adherence to planned future experiments, patterns were generated as white speckles on a black background.

When creating patterns, two different parameters were altered: positional randomness and speckle shape. Positional randomness varied at 0%, 50% and 100%, with 0% randomness being a uniform grid of dots and 100% being a fully randomized spread of speckles. A nominal grid of speckles was created from speckle spacing, size and spacing to decide position. Then, deviation from the grid point was determined based on desired randomness, with more randomness resulting in farther deviations from grid points.

Multiple shape geometries were used to assess the robustness of the patterns. Regular, or box, speckles were the first shape tested; these were uniform square dots with consistent area and boundaries. Irregular, or cross, speckles were also used, which are symmetric shapes with consistent area, but irregular boundaries. The last shape case involved a variety of speckle shapes – crosses, L-shapes, and zig-zag geometries – to represent extreme non-uniformity, with the proportion of each shape in the pattern being chosen randomly using a normal distribution. Speckle density and spacing were decided to ensure that pattern coverage remained as close to 50% as possible to maximize contrast, which was kept uniform for all patterns. All experimental combinations may be seen in Table 1.

Strain was incrementally applied to patterns, based on the input desired number of output images, by identifying coordinates with white ink and multiplying these coordinates by a deformation tensor to get the new location of the speckles, seen as follows [14].

$$\begin{bmatrix} 1+\varepsilon_{xx} & \gamma_{xy} \\ \gamma_{yx} & 1+\varepsilon_{yy} \end{bmatrix} \begin{pmatrix} x_{init} \\ y_{init} \end{pmatrix} = \begin{pmatrix} x_{final} \\ y_{final} \end{pmatrix}$$

Table 1 All speckle pattern parameter combinations tested, in which placement randomness and speckle shape were varied. All other parameters were consistent across tests.

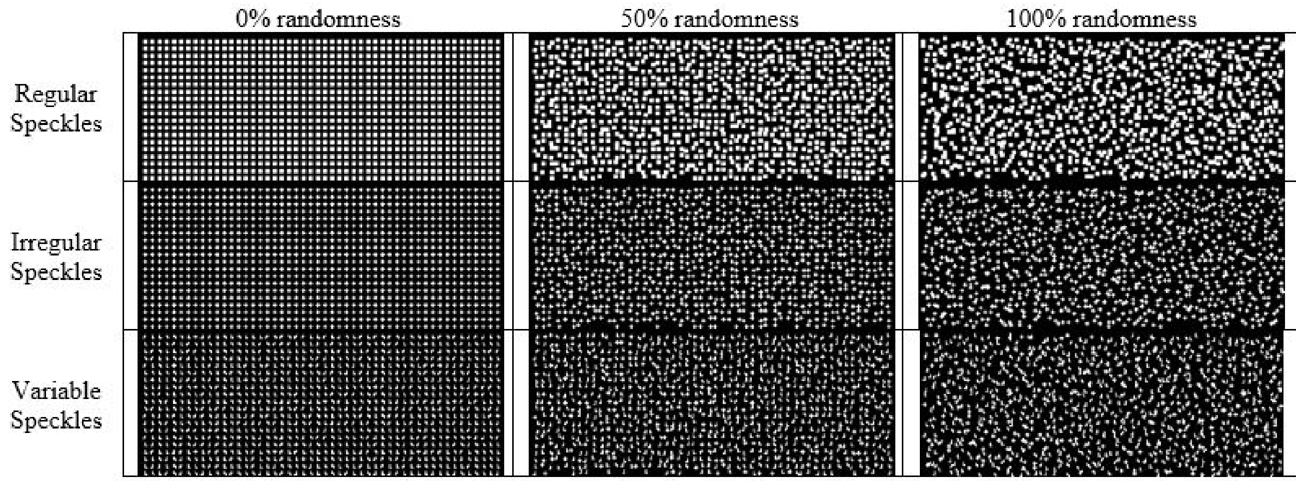

The deformation tensor for each of the seven strain states, along with a brief description, may be found in Table 2. Tensors were divided by the desired number of output images to create steps with which to apply incremental deformation to the pixel locations.

Table 2 All strain state final deformation tensors. Coordinates containing white pixels were multiplied by the tensors to output their new locations under each strain state.

10% tensile strain along x (ε_{tx})	10% compressive strain along x (ε_{cx})	Biaxial tensile strain, 10% along x, 5% along y ($2\varepsilon_{tx} : \varepsilon_{ty}$)	Biaxial tensile strain, 10% along both x and y ($\varepsilon_{tx} : \varepsilon_{ty}$)	10% tensile strain along x and 0.087 radian shear strain along x (ε_{tx} & γ_x)	0.087 radian shear strain along x (γ_x)	0.087 radian shear strain along y (γ_y)
$\begin{bmatrix} 1.1 & 0 \\ 0 & 1 \end{bmatrix}$	$\begin{bmatrix} 0.9 & 0 \\ 0 & 1 \end{bmatrix}$	$\begin{bmatrix} 1.1 & 0 \\ 0 & 1.05 \end{bmatrix}$	$\begin{bmatrix} 1.1 & 0 \\ 0 & 1.1 \end{bmatrix}$	$\begin{bmatrix} 1.1 & 0.087 \\ 0 & 1 \end{bmatrix}$	$\begin{bmatrix} 1 & 0.087 \\ 0 & 1 \end{bmatrix}$	$\begin{bmatrix} 1 & 0 \\ 0.087 & 1 \end{bmatrix}$

Testing & Analysis

The computationally deformed patterns were evaluated using VIC-2D 7 to appraise their accuracy and precision under known deformation levels. A comparison of pattern performance across parameters would then offer insight into the combinations that provide the most accurate and least uncertain strain measurements. A subset size of 29 pixels was used with a step size of 7 pixels, as recommended by VIC-2D, to calculate the Lagrangian strain of each test. Figure 1 shows an example of a pattern before deformation, after deformation, and after analysis.

The performance of each pattern under each applied strain state was evaluated using the aggregate statistics of each test analysis, particularly the mean strain values for axial strain in both directions and shear on the XY plane and the standard deviation of these values, a measure of how distant each localized strain calculation was from the global value.

To quantify accuracy, theoretical strain tensors, created from expected strain values for each case, were compared with experimental deformation tensors created using analysis data. For the final frame of each analysis, the theoretical and experimental strain tensors were defined as follows.

$$E_{theory} = \begin{bmatrix} e_{xx,t} & e_{xy,t} \\ e_{yx,t} & e_{yy,t} \end{bmatrix} \qquad E_{exp} = \begin{bmatrix} e_{xx,e} & e_{xy,e} \\ e_{yx,e} & e_{yy,e} \end{bmatrix}$$

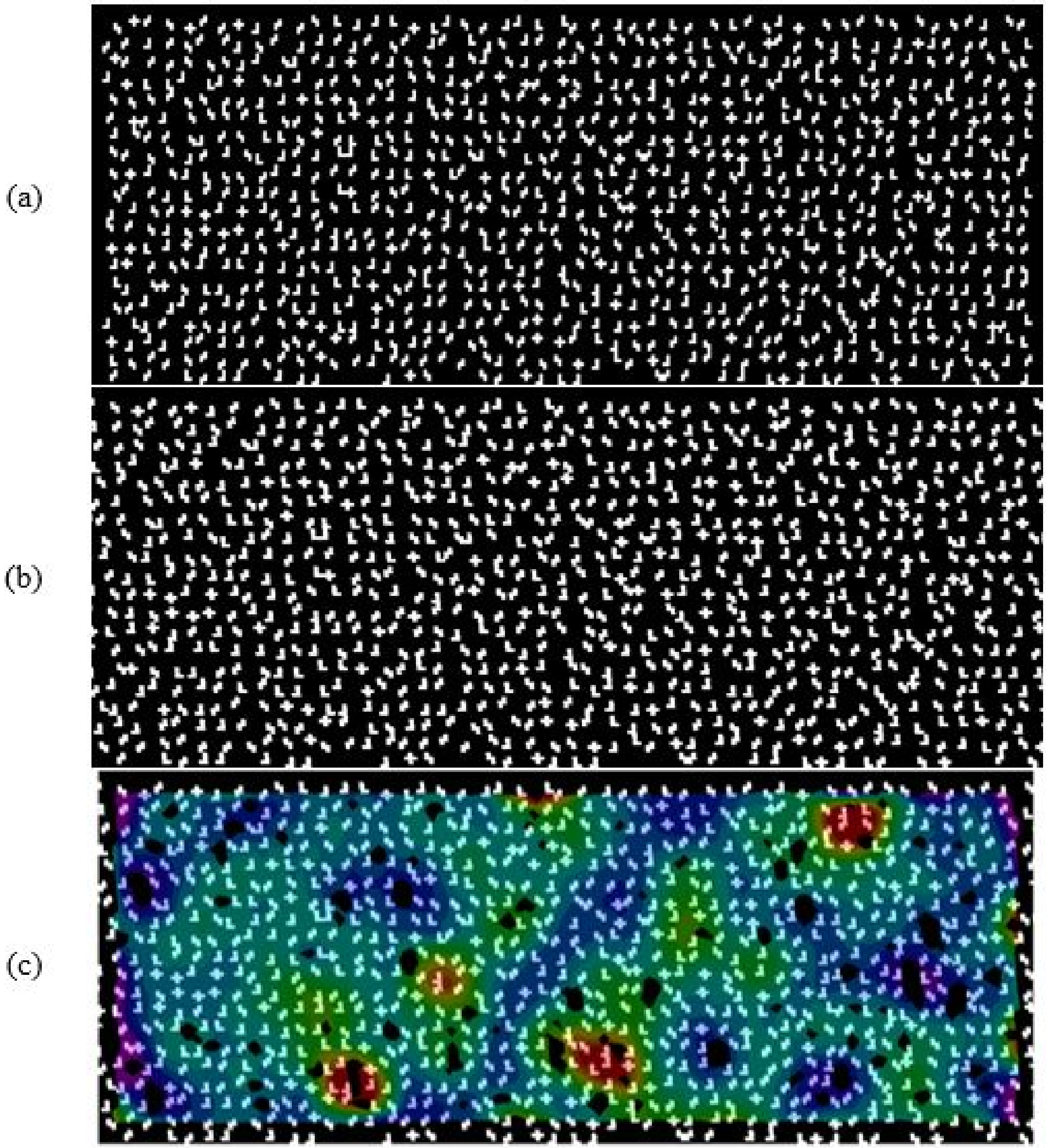

Fig. 1 A speckle pattern with variable speckles and 50% randomness after 10% tensile strain along x with 0.087 radian shear strain along x deformation was applied and then analyzed. (a) shows the image prior to being deformed, (b) shows the image after being deformed, and (c) shows the image after being analyzed.

The error tensor was then defined by the following equation.

$$\Delta E = \begin{bmatrix} e_{xx,t} & e_{xy,t} \\ e_{yx,t} & e_{yy,t} \end{bmatrix} - \begin{bmatrix} e_{xx,e} & e_{xy,e} \\ e_{yx,e} & e_{yy,e} \end{bmatrix} = \begin{bmatrix} E_{xx} & E_{xy} \\ E_{yx} & E_{yy} \end{bmatrix}$$

The final error of each pattern measurement was obtained by taking the Frobenius norm of the final error tensor.

Variability, as a metric of the spread of localized deformation calculations, was calculated by propagating the standard deviations reported.

$$U = \sqrt{(\sigma_{xx})^2 + (\sigma_{yy})^2 + (\sigma_{xy})^2 + (\sigma_{yx})^2}$$

Results

The error of each test as a percentage of the target strain value may be seen in Table 3. Irregular speckles performed the best for axial strain states, with regular speckles also performing well. For regular and irregular speckles, no significant correlation between randomness and performance for axial strain states was noticed except for 1:1 biaxial tension, in which patterns with 0% randomness performed particularly worse. No pattern performed well for any applied shear value. Variable speckles showed acceptable accuracy at most axial strain values for 50-100% randomness, but there was noticeably poor performance across the table for patterns with 0% randomness.

Table 3 Percent error of mean calculated strain relative to theoretical strain for all pattern combinations, varying speckle shape and orientation, and strain states. Color grading highlights performance, as lower values indicate higher accuracy, with green being the most accurate and red being the least.

		ε_{tx}	ε_{cx}	$2\varepsilon_{tx} : \varepsilon_{ty}$	$\varepsilon_{tx} : \varepsilon_{ty}$	ε_{tx} & γ_x	γ_x	γ_y
Regular Speckles	0% randomness	0.76%	1.93%	2.02%	53.42%	14.14%	13.80%	13.87%
	50% randomness	1.26%	1.63%	1.20%	1.64%	15.00%	13.87%	14.09%
	100% randomness	1.37%	1.34%	1.48%	1.89%	14.85%	15.13%	14.54%
Irregular Speckles	0% randomness	0.37%	0.76%	1.28%	14.14%	14.30%	13.57%	13.56%
	50% randomness	1.26%	0.97%	1.48%	1.20%	14.48%	13.71%	13.82%
	100% randomness	1.42%	0.26%	0.69%	1.21%	14.66%	13.72%	13.79%
Variable Speckles	0% randomness	24.78%	13.93%	19.69%	38.32%	18.02%	13.77%	13.84%
	50% randomness	1.72%	13.75%	1.44%	1.68%	14.74%	13.88%	13.87%
	100% randomness	2.15%	13.63%	2.28%	2.73%	14.92%	14.21%	13.79%

The standard deviations of localized strains as percentages of the target strain value are shown in Table 4. Across the board, the irregular speckles showed more stability than either of the other speckle groups - at all randomness levels, strain standard deviation remained below 2.5%. Regular and variable speckles both had cases of standard deviations above 100% and consistently had values above 3%. For these two pattern types, patterns with 0% randomness had noticeably poor consistency, with consistency improving significantly with the introduction of placement randomness.

Table 4 Standard deviations of calculated strain normalized by the target strain value for all pattern combinations, varying speckle shape and orientation, and strain states. Color grading highlights performance, as lower values indicate higher consistency, with green being the most consistent and red being the least.

		ε_{tx}	ε_{cx}	$2\varepsilon_{tx} : \varepsilon_{ty}$	$\varepsilon_{tx} : \varepsilon_{ty}$	ε_{tx} & γ_x	γ_x	γ_y
Regular Speckles	0% randomness	1.56%	2.14%	3.19%	*116.30%*	2.69%	0.90%	0.82%
	50% randomness	1.33%	1.13%	1.55%	2.23%	4.96%	4.69%	3.56%
	100% randomness	1.33%	0.92%	1.76%	1.68%	5.42%	8.34%	4.63%
Irregular Speckles	0% randomness	1.02%	1.49%	1.63%	0.00%	2.38%	0.50%	1.79%
	50% randomness	1.48%	1.18%	1.48%	1.52%	1.37%	0.77%	0.74%
	100% randomness	2.22%	1.88%	2.04%	2.80%	1.84%	1.22%	1.51%
Variable Speckles	0% randomness	*122.28%*	0.52%	*225.54%*	*118.07%*	19.30%	3.08%	0.58%
	50% randomness	1.61%	0.76%	1.47%	1.69%	3.39%	5.95%	1.11%
	100% randomness	2.30%	1.23%	2.50%	2.74%	3.66%	4.53%	1.65%

Patterns were physically printed onto aluminum, the planned experimental test material, spray painted black. Looking at the printed speckles, which may be seen in Figure 2, under a microscope revealed that speckles that were designed to be square digitally exhibited ink bleeding when printed, resulting in distorted edges and higher-than-anticipated white coverage.

Discussion

Speckle shape plays an important role in both the accuracy and precision of DIC pattern performances – dependency is case specific but has the potential to be large. Some cases show that randomness does influence accuracy, but overall, it has a more

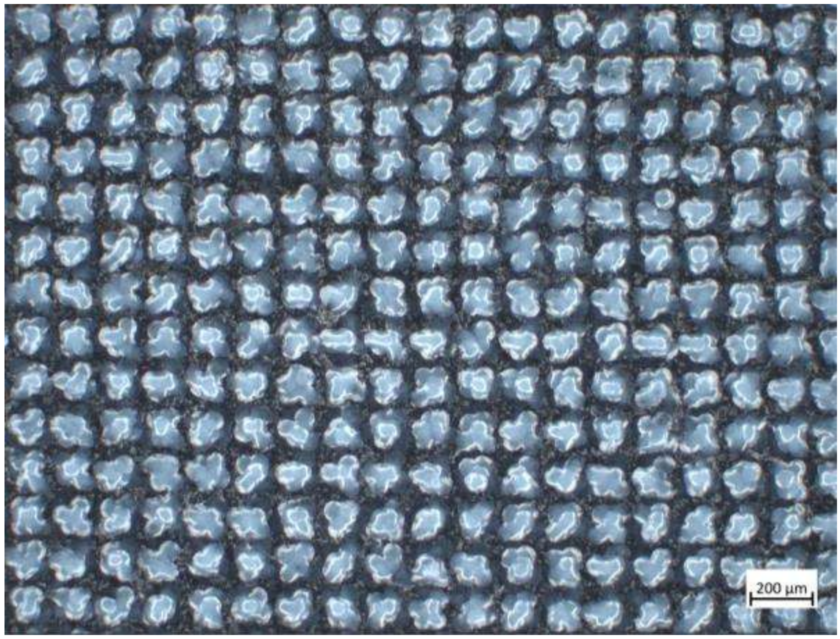

Fig. 2 Printed speckle patterns, intended to be perfect squares, under a microscope to highlight ink spreading and shape irregularities.

significant effect on precision, while the reverse is true for speckle shape. Regular speckles have high accuracy for most axial strain states, except for the 0% randomness pattern and 1:1 biaxial tension strain state. Unexpectedly, randomness had little effect on the error of the strain measurement. Variable speckles introduce significant mean error and error variability in axial strain cases unless adequate randomness is applied, in which case their performance approaches that of irregular speckle patterns. Overall, irregular speckles with non-zero randomness performed the best, providing both accuracy and precision across axial strain states.

Shear strain error was high across all patterns and all stress states, with error values consistently above 13%. This discrepancy indicates that the current computational modeling process may be representative of a DIC setup with too low of a camera resolution to accurately measure shear deformation. One potential improvement, therefore, could be to increase the magnification of the patterns, allowing for better tracking of diagonal displacements.

Overall, the results support the notion that the performance and stability of the strain measurements are roughly correlated with the type of speckles used and the position of the speckles. Irregular speckle patterns with any degree of randomness performed the best overall, showing that irregularity in pattern form improves the robustness of strain measurements. The variability in reported strains worsened across the board for irregular and variable speckle shapes when evaluating 100% random patterns, as compared to 50% random patterns, with no significant impacts on accuracy. Even with regular speckle shapes, no remarkable gains were made in precision when going from 50% to 100% randomness. Patterns with no randomness had remarkably high rates of variability, meaning the strain measurements are unreliable, even with the density of available information.

The bleed of the ink on UV printed test samples suggests that printing patterns may inherently impact the speckle density and randomness of the pattern by introducing randomness in pixel shape, which has the potential to introduce sufficient variability to reach the desired degree of randomness. It remains unknown whether randomness in speckle orientation or shape is necessary – if UV printing the patterns introduces sufficient variability through imperfections caused by ink spreading, the need for deliberate positional randomness may be deemed unnecessary, allowing for higher pixel density and improved analytical resolution.

Conclusion

The results prove that both speckle shape and positional randomness play roles in the optimization of speckle patterns when used in axial strain cases. The accuracy of measurement from a speckle pattern shows a dependence on speckle shape, with speckles of any standardized shape outperforming variable speckle shapes. The precision of measurement is influenced by the position of the speckles, with positional randomness of any sort decreasing the deformation measurement variability. The degree of randomness, beyond 50%, had little additional benefit, and in fact increased the likelihood of large areas of uniform color, which decreases the amount of information to be derived from that area. Tests with shear strain were inaccurate, indicating the need for higher camera resolution and magnification in future tests.

Printing patterns onto aluminum blanks using a UV printer revealed that the printing process can inherently introduce variability in patterns, which can be utilized to replace positional randomness, possibly improving data density by allowing grids of dots to be used in patterns. Future work will explore the limits and benefits of UV printing for repeatable, customizable, and inherently random speckle patterns at small scales with large camera magnification, allowing the variation in speckles to be seen. Physical validation of selected tensile and shear patterns on aluminum samples will be used to corroborate computational findings, with emphasis during testing and analysis on the effects of magnification, subset size, and step size to improve measurement accuracy

References

1. Sutton, Michael A.; Orteu, Jean-J; Schreier, Hubert W. *Image Correlation for Shape, Motion and Deformation Measurements: Basic Concepts, Theory and Applications.* Springer, 2009.
2. Pan, Bing. "Digital Image Correlation for Surface Deformation Measurement: Historical Developments, Recent Advances and Future Goals." *Measurement Science and Technology* **29**(8), 082001 (2018).
3. Bogusz, Paweł; et al. "Application of Digital Image Correlation for Strain Mapping, Displacement, and Deformation Measurement." *PMC – National Institutes of Health (PMC11174112)*, 2024.
4. Liu, X.-Y.; Li, R.-L.; Zhao, H.-W.; et al. "Quality Assessment of Speckle Patterns for Digital Image Correlation by Shannon Entropy." *Optik* **126**(23), 4206–4211 (2015).
5. Park, J.; Yoon, S.; Kwon, T.-H.; et al. "Assessment of Speckle-Pattern Quality in Digital Image Correlation Based on Gray Intensity and Speckle Morphology." *Optics and Lasers in Engineering* **91**, 62–72 (2017).
6. Correlated Solutions, Inc. *Speckle Pattern Fundamentals.* Application Note, VIC-3D 9, 2021.
7. Dong, Y. L.; Pan, B. "A Review of Speckle Pattern Fabrication and Assessment for Digital Image Correlation." *Experimental Mechanics* **57**(8), 1161–1181 (2017).
8. Pan, B.; Xie, H.; Wang, Z.; et al. "Study on Subset Size Selection in Digital Image Correlation for Speckle Patterns." *Optics Express* **16**(10), 7037 (2008).
9. Zhang, Juan; Sweedy, Ahmed; Gitzhofer, François; Baroud, Gamal. "A Novel Method for Repeatedly Generating Speckle Patterns Used in Digital Image Correlation." *Optics and Lasers in Engineering* **100**, 259–266 (2018).
10. Weissman, Clifford. "Non-Contact 3D Deformation and Strain Measurements Using Digital Image Correlation for Biomedical Applications." *Biomechanics* **2018** (2018).
11. Wang, Y.; Gao, Y.; Liu, Y.; Gao, Z.; Su, Y.; Zhang, Q. "Optimal Aperture and Digital Speckle Optimization in Digital Image Correlation." *Experimental Mechanics* **61**, 677–684 (2021).
12. Kramer, Sharlotte; Reu, Phillip; Bonk, Sarah. *A Speckle Patterning Study for Laboratory-Scale DIC Experiments.* Sandia National Laboratories, Albuquerque, NM, USA, 2017.
13. Roland DG Corporation. *VersaUV LEF-12i Benchtop UV Flatbed Printer: Specifications.* 2020. Retrieved from https://www.rolanddga.com
14. Rudnicki, John W. *Fundamentals of Continuum Mechanics.* John Wiley & Sons, 2014.